

Volumetric Analysis of Endoscopic and Maxillary Swing Surgical Approaches for Nasopharyngectomy

Nidal Muhanna^{1,2,3} Harley Chan¹ Jimmy Qiu¹ Michael Daly¹ Tahsin Khan¹ Francesco Doglietto⁴
Walter Kucharczyk^{1,5} David P. Goldstein^{2,3} Jonathan C. Irish^{1,2,3} John R. de Almeida^{1,2,3}

¹TECHNA Institute, University Health Network, Toronto, Ontario, Canada

²Department of Surgical Oncology, Princess Margaret Cancer Centre, Toronto, Ontario, Canada

³Department of Otolaryngology – Head & Neck Surgery, University of Toronto, Toronto, Ontario, Canada

⁴Department of Neurosurgery, University of Brescia, Owensboro, Kentucky 42301, United States

⁵Department of Medical Imaging, Toronto General Hospital, Toronto, Ontario, Canada

Address for correspondence John de Almeida, MD, MSc, FRCSC, Department of Otolaryngology - Head and Neck Surgery, University Health Network, Princess Margaret Cancer Centre, 610 University Ave., 3-955, Toronto, ON M5G 2M9, Canada (e-mail: john.dealmeida@uhn.ca).

J Neurol Surg B 2018;79:466–474.

Abstract

Objectives/Hypothesis The endoscopic endonasal approach (EEA) for nasopharyngectomy is an alternative to the maxillary swing approach (MSA) for selected recurrent nasopharyngeal carcinomas (NPC). We compare the access between these approaches.
Methods Three cadaver specimens were used to compare access volumes of the EEA and MSA. Exposure volumes were calculated using image guidance registration to cone beam computed tomography and tracking of accessible tissue with volumetric quantification. The area of exposure to the carotid artery was measured.

Results The MSA provided higher volumes for access volume compared with the EEA (66.6 vs 39.1 cm³, $p = 0.009$). The working area was larger in the MSA (80.2 vs 56.9 cm², $p = 0.06$). The exposure to the carotid artery was higher in the MSA (1.88 vs 1.62 cm², $p = 0.04$). The MSA provided larger volume of exposure for tumors of the parapharyngeal space with exposure below the palate.

Conclusions This study suggests that the MSA for nasopharyngectomy provides a larger volume of exposure. However, much of the increased exposure relates to exposure of the parapharyngeal space below the palate. The EEA provides adequate access to superior anatomical structures.

Keywords

- ▶ endoscopic
- ▶ maxillary swing
- ▶ exposure volume
- ▶ image guidance
- ▶ nasopharyngectomy

Introduction

Although nasopharyngeal carcinoma (NPC) is a relatively rare subset of head and neck carcinomas (HNCs) in most countries, its anatomical proximity to critical structures presents a therapeutic challenge. For early stages of the disease (T1-T2), radiation therapy is the primary course of treatment, while concurrent chemotherapy is typically employed for advanced stages (T3-T4) of NPC.^{1,2} However, local recurrence rates range from 9% to 40%, thus requiring additional treatments.^{3–5}

For recurrent cases, treatment options include surgical salvage with nasopharyngectomy or reirradiation. Nasopharyngectomy is associated with improved local control and overall survival compared with reirradiation.^{6–8} However, the proximity of the nasopharynx to critical anatomical structures (e.g., internal carotid artery, optic nerve, brain stem, and pituitary–hypothalamic axis) often limits surgical access and impacts surgical resectability. A variety of surgical approaches have been used to access the nasopharynx including transpalatal, transmaxillary/transantral, and maxillotomy approaches.^{9–11}

received

October 14, 2016

accepted after revision

November 10, 2017

published online

January 19, 2018

© 2018 Georg Thieme Verlag KG
Stuttgart · New York

DOI <https://doi.org/10.1055/s-0037-1617432>.
ISSN 2193-6331.

However, these open surgical procedures are associated with potential complications such as palatal fistulas, trismus, dysphagia, and nasal regurgitation.⁹ In one study, 54% of patients with an open approach suffered postoperative complications.¹⁰

The endoscopic endonasal approach (EEA) has been used as a less invasive alternative to traditional external approaches for the management of residual/recurrent NPC.^{12–18} This approach is associated with shorter postsurgical recovery times and evades external facial incisions.¹⁹ However, no studies have compared the access to the nasopharynx using this approach and traditional approaches. The objective of this study was to compare surgical access to the nasopharynx using either the EEA or maxillary swing (MS) surgical approach. We developed and utilized novel quantitative and tracking methods to estimate surgical exposure volumes using computed tomography (CT) assessment. This investigation provides insight into critical differences between both surgical approaches to determine the conditions where each method may be most suitable.

Materials and Methods

Definitions of Parameters

1. **Volume:** Three-dimensional (3D) space available in craniocaudal, anterior–posterior, mediolateral dimensions, for the free movement of surgical instruments; synonymous with “surgical access volume” or “surgical window.” In our study, the anterior border of the access volume was defined behind the posterior septum.
2. **Deep surface area:** Two-dimensional (2D) space that is at the level of the surgical target (i.e., the deepest surface area that can or must be accessible).
3. **Working surface area:** Although often synonymous with deep surface area, we designated this term to include the surface area from the entry point of surgical instruments to the area that is at the level of the surgical target

Study Design

Under University Health Network institutional Research Ethics Board approval, three human head cadaveric specimens were acquired from Department of Anatomy at the University of Toronto for research study. The specimens were sectioned through the neck and preserved in a refrigerator at -10°C prior to proceeding with the study. Inspection of the cadavers was first conducted using a prototype cone-beam computed tomography (CBCT) scanner to review the cadavers' internal structure. The nasal aperture in each cadaver was visualized endoscopically using a 0° telescope (Karl Storz Hopkins II and IMAGE1 Camera; Karl Storz, Tuttlingen, Germany). All three specimens were free of diseases, previous surgical procedures, and/or malignant structures. An Otolaryngology Head and Neck Surgeon specialized in Endoscopic Skull Base Surgery and Open Head and Neck Surgery and a surgical fellow conducted two procedures for each specimen: (1) endoscopic nasopharyngectomy on right side followed by (2) open MS approach on left side of the specimen. Two CBCT scans were acquired for each specimen—(1) a preoperative scan for inspection and (2) a postoperative scan

after both MS and EEA procedures for surgical access volume measurement. To measure surgical access volume, an in-house navigation/visualization software (GTxEyes) was employed, along with commercially available optical tracking hardware.

Maxillary Swing Procedure

For the MS procedure, a Weber-Ferguson skin incision was made in the mid-lid region beneath the lower lash-line following the lateral nasal process to the base of ala and continuing to the base of the columella. At this point, the vertical incision from the columella was continued inferiorly to the vermilion border of the lip with a full-thickness incision of the upper lip at the level of the central incisors. A palatal incision was made along the inner surface of the alveolar ridge and a palatal mucosal flap was lifted to past the midline. After exposing bone for all necessary osteotomies, four bone cuts were made. The first osteotomy spanned horizontally at the level of the inferior margin of the infra-orbital foramen, from the pyriform aperture medially to the malar aspect of the zygoma laterally. A second osteotomy was made from the inferior aspect of the pyriform aperture superiorly to between the central incisors inferiorly. The third osteotomy was made in an anterior to posterior direction through the midline of the hard palate. Finally, an osteotomy from the posterior hard palate cut laterally to the back of the maxillary tuberosity and the maxilla was released from the pterygoid plates using a curved osteotome. The entire hemi maxilla was then swung laterally on a soft tissue pedicle to access the nasopharynx.

Endoscopic Approach Procedure

The navigation system (optical tracking system) was used during this procedure and was located in front of the surgeons above head level to avoid line of sight issues. The primary surgeon performed resection tasks in one hand while holding the surgical suction in the other hand. The assistant surgeon was positioned at the head of the bed and provides endoscopic visualization and irrigation. The navigation system registered to CBCT imaging was used on demand per surgeon request with a tracked pointer. Per standard operation protocol, expansion of the natural nasal corridor constituted (1) ipsilateral middle turbinectomy, (2) anterior and posterior ethmoidectomies, (3) enlargement of a natural antrostomy to the posterior maxillary sinus wall, (4) removal of the posterior maxillary sinus wall and lateralization of the pterygopalatine fossa contents, (5) drilling of the pterygoid wedge and pterygoid plates, (6) a posterior nasal septectomy, (7) bilateral wide sphenoidotomies; and removal of the floor of the sphenoid sinuses to the level of the clivus. A high-speed drill with a 3- or 4- mm diamond burr was used to remove bone if needed.

CBCT Imaging

A prototype mobile CBCT C-arm was employed for this study and was developed in collaboration with Siemens Healthcare (Erlangen, Germany). C-arm modifications included a flat-panel detector (Paxscan 4030CB, Varian, Palo Alto, California, United States), motor-driven rotation,

geometric calibration method, and in-house developed software control system. Volumetric images covering a field of view of $20 \times 20 \times 15\text{cm}^3$ were reconstructed within 15 seconds of scan completion using the FDK filtered back-projection method.²⁰ Acquisition of images by the scanner was 1 minute long, capturing 200 projections around the object from 0 to 178 degrees. The reconstruction volume consisted of 192 axial slices with 256×256 pixels; the voxel size is isotropic 0.78mm^3 .

Optical Tracking System

An optical tracking system (Polaris, Northern Digital, Waterloo, Ontario, Canada) provided 6 degrees of freedom (DoF) (x, y, z, pitch, yaw, roll) tracking and navigation with respect to the CBCT images. Rigid registration of the optical tracking system to the CBCT was performed using standard donut-shaped fiducial skin markers (IZI Medical, Baltimore, Maryland, United States) and in-house software developed using open source toolkits including the Image Guided Surgery Toolkit (IGSTK),²¹ Visualization Toolkit (VTK),²² and Insight Segmentation and registration Toolkit (ITK).²³ The navigation system software platform GTxEyes provides a surgical dashboard with orthogonal 2D CT viewing planes (axial, sagittal, coronal), 3D CBCT surface reconstruction, and a feed of the endoscopic video stream.^{24–26}

An optical pointer tool with six DoF was used to navigate the 2D and 3D views in real time. The tip of the tool was used to reslice the axial, sagittal, and coronal planes. 2D projections of the optical tool were overlaid on top of each 2D viewing plane. In the 3D view, the position and orientation of the tool were shown with respect to the CBCT surface reconstruction.

Volume Visualization and Measurement

CBCT images were collected for each specimen pre-exposure as well as after the MS and EEA exposures. Following registration of the optical system to the postoperative CBCT images, recordings of an optical pointer tool were

collected while tracing out the superficial and the deep surfaces of the exposures.

For each surgical approach under evaluation, the pointer probe was used to trace out the boundaries of the accessible volume postexposure. This simulated the access provided by nonangled surgical instruments for each approach. The optical navigation system recorded measurements of the approach collected by the tip of the pointer probe during tracing. Delaunay triangulation was then applied on the set of recorded measurements to generate a 3D model of the accessible volume of the approach. The generated volumes were rendered with the CBCT surface reconstruction for 3D viewing. For the 2D projections, the 3D volumes were resliced by the current axial, sagittal, and coronal planes defined by the tip of the optical pointer. The resulting 2D exposures were then overlaid on top of the axial, sagittal, and coronal slices. The recorded tip positions and surface models for the evaluated approaches were stored for offline review and analysis.

The volumes of the exposures were calculated using the finite volume method applied to the triangulated exposure.²⁴ Mean and standard deviation were calculated for the MS and EEA volumes. The soft palate plane was defined in the sagittal view. The MS and EEA volumes were then split in two along the soft palate plane.

Similarly, for the lateral and medial volumes, a split plane was defined in the axial view on the left and right side across the medial pterygoid plate. The planes were used to split the MS and EEA volumes in two.

Surface Measurement

For the surface area, areas of the triangles that make up the 3D model of the accessible were summed to calculate the working surface area. A deep plane was defined by the surgeon beyond which the tracked pointer reached the level of the surgical target. The deep surface area was calculated by summing the areas of the triangles beyond the defined plane. Mean and standard deviation were calculated for the work-

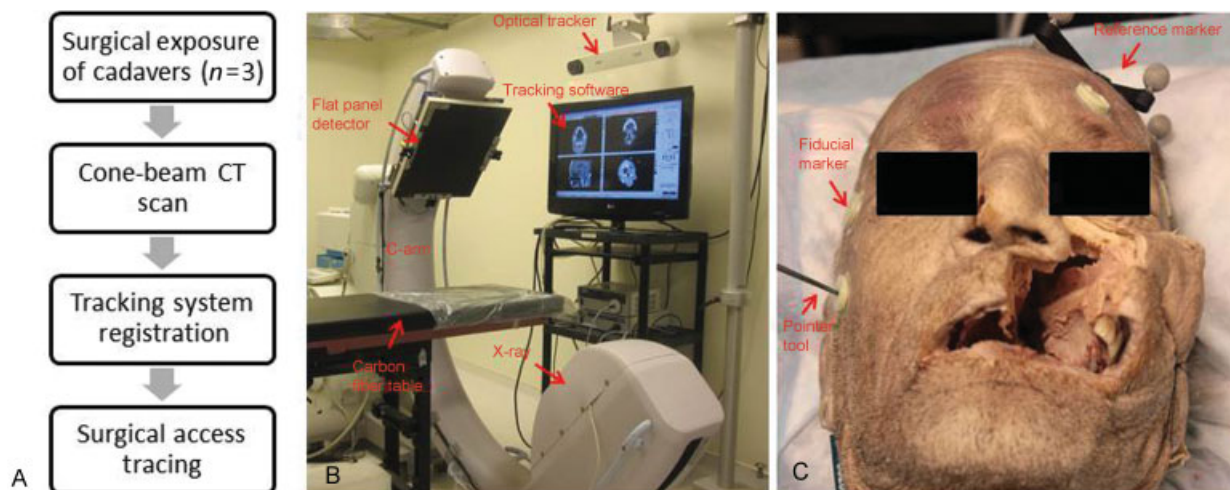


Fig. 1 Illustration of the study work flow. (A) Flow chart of experimental protocol showing an overview of study design. (B) Experimental setup with cone-beam computed tomography (CT) and optical tracker. (C) Representative cadaver specimen on the carbon fiber table with fiducial markers on its surface and reference marker tracked by the optical tracker.

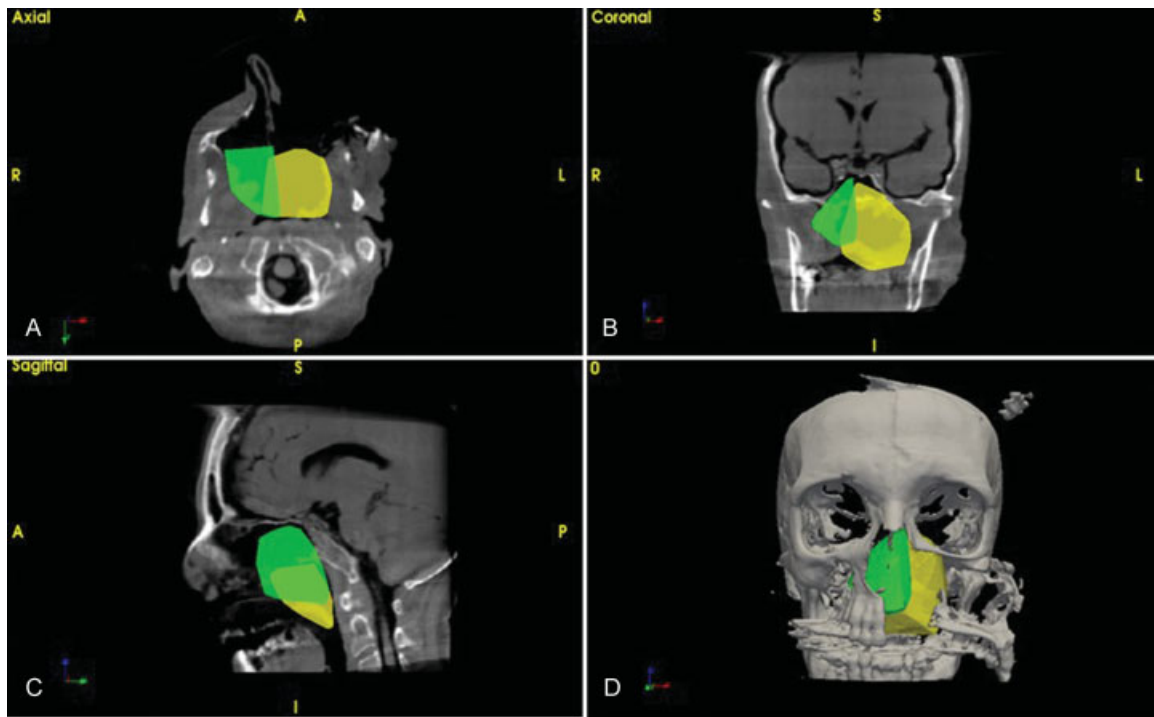


Fig. 2 Surgical access volumes for endoscopic endonasal (green) and maxillary swing (yellow) approaches. (A) Two-dimensional visualization of access volumes in cone-beam computed tomography axial, (B) coronal, (C) sagittal slices, and (D) three-dimensional reconstruction and surgical volume. A: anterior, P: posterior, S: superior, I: inferior, R: right, L: left.

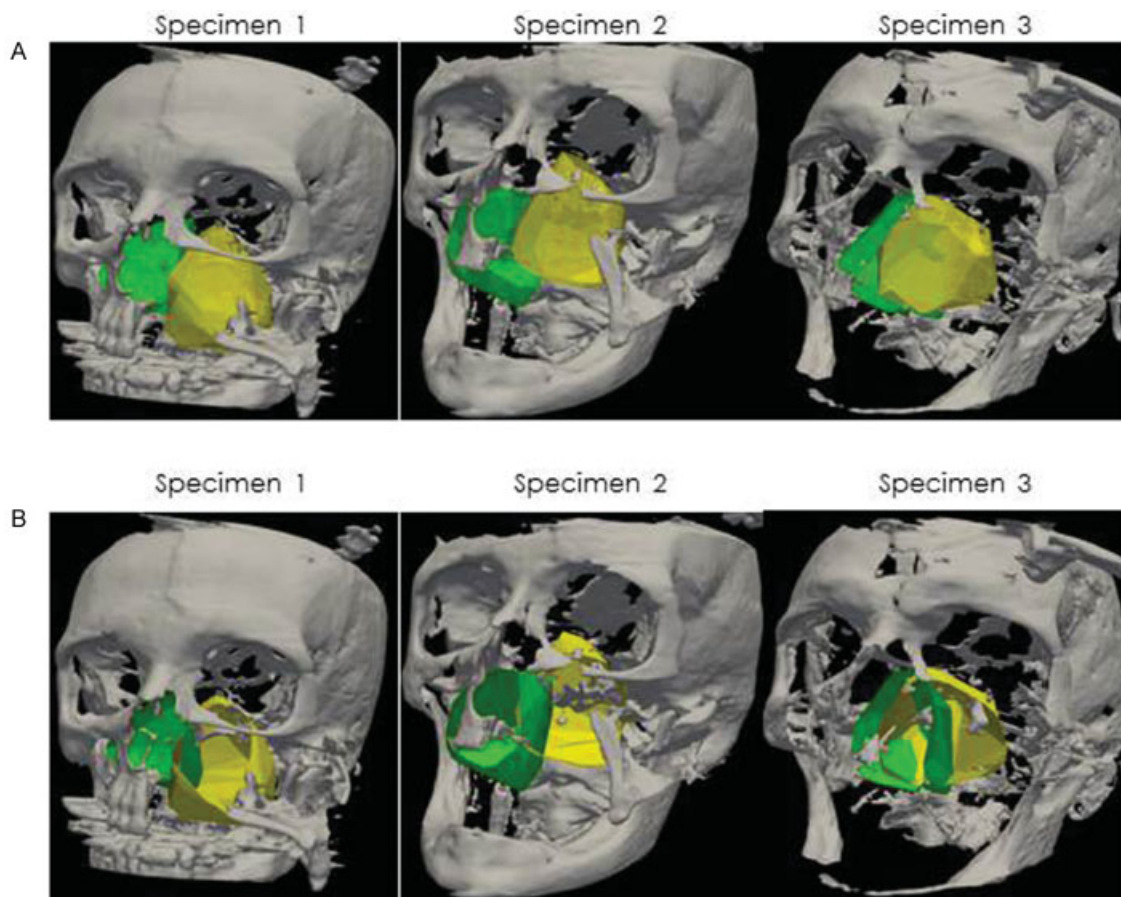


Fig. 3 (A) Three-dimensional (3D) visualization of access volumes in 3D surface model for endoscopic endonasal (green) and maxillary swing approaches (yellow), and (B) 3D visualization surface area 3D surface model for three different specimens.

This document was downloaded for personal use only. Unauthorized distribution is strictly prohibited.

ing surface area and deep surface area of MS and EEA exposures.

Carotid Surface Measurement

Similar to the MS and EEA exposures, the left and right parapharyngeal carotids were traced out using the tracked pointer. We chose the parapharyngeal carotid artery as this is the portion often relevant in nasopharyngectomy surgical cases and as such we quantified these. Measurements of the left and right carotid were calculated based off the triangulated carotid volumes, where the areas were determined by summing the areas of the surface triangles.

Results

Fiducial markers were placed on each specimen prior to obtaining imaging studies (either pre- or postoperative CBCT (**►Fig. 1A**)). An NDI Polaris optical tracking system was used for both registration and tracking. Registration was completed using the tracking device to identify known fiducial markers after obtaining CBCT scans (**►Fig. 1B**). The tracking device was then used for quantification of surgical exposure by manual tracing of accessible surgical areas using either

the EEA or MS approach. Delaunay triangulation was applied on the pointer measurements to create 3D polygonal representations of the exposure contours to create 3D exposure volumes. Quantitative endoscopic tracking and video overlay enabled retrospective contouring of the surgical exposure volume. **►Fig. 1C** illustrates a representative cadaver specimen with fiducial markers after both EEA and MS nasopharyngectomy procedures were conducted.

Three cadaver specimens underwent both EEA nasopharyngectomy through the right nostril, followed by the MS nasopharyngectomy on the left side. Comparison of exposure volumes demonstrates that the MS approach has greater surgical access compared with the endoscopic approach across all three specimens (**►Figs. 2 and 3**). 2D sections representative of a cadaver skull clearly indicate that the MS approach enables larger lateral access compared with the EEA, although further attempts to determine what regions gained better access did not yield any further detail (**►Fig. 4**). Moreover, the MS approach appears to enable greater surgical access volume on the inferior aspect of the nasopharynx, and provides greater access volume on the superior aspect of the sphenoid sinus (**►Fig. 5**). Our observation revealed that there was a qualitative improvement in visualization of

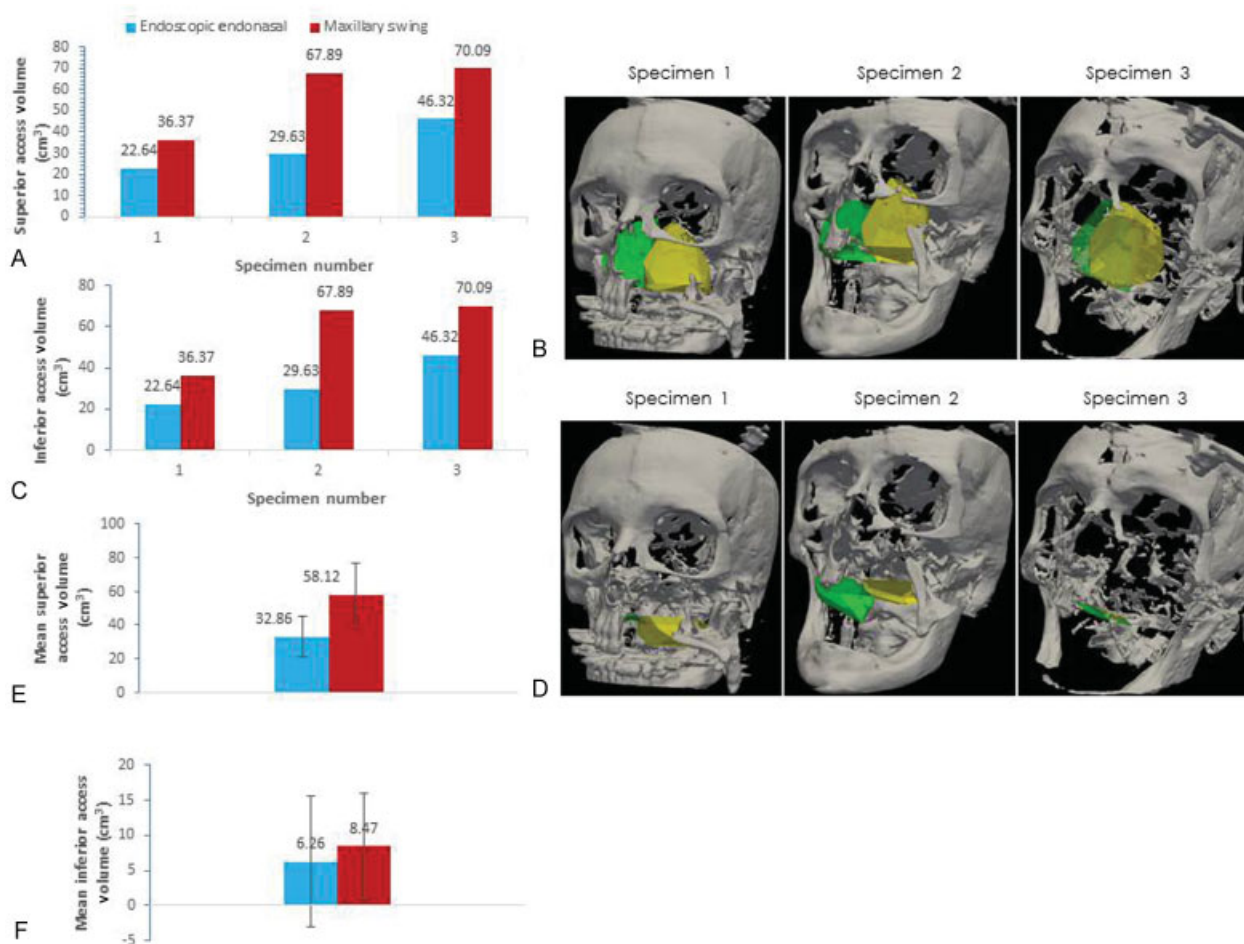


Fig. 4 (A) Superior surgical access volumes split at the soft palate and (B) three-dimensional (3D) visualization of superior access volumes split at soft palate in 3D surface model for endoscopic endonasal (green) and maxillary swing approaches (yellow). (C) Inferior surgical access volumes for endoscopic endonasal and maxillary swing approaches and (D) 3D visualization of inferior access volumes of 3D surface model for three different specimens. (E) Mean superior volume and standard deviation and (F) mean inferior volume and standard deviation.

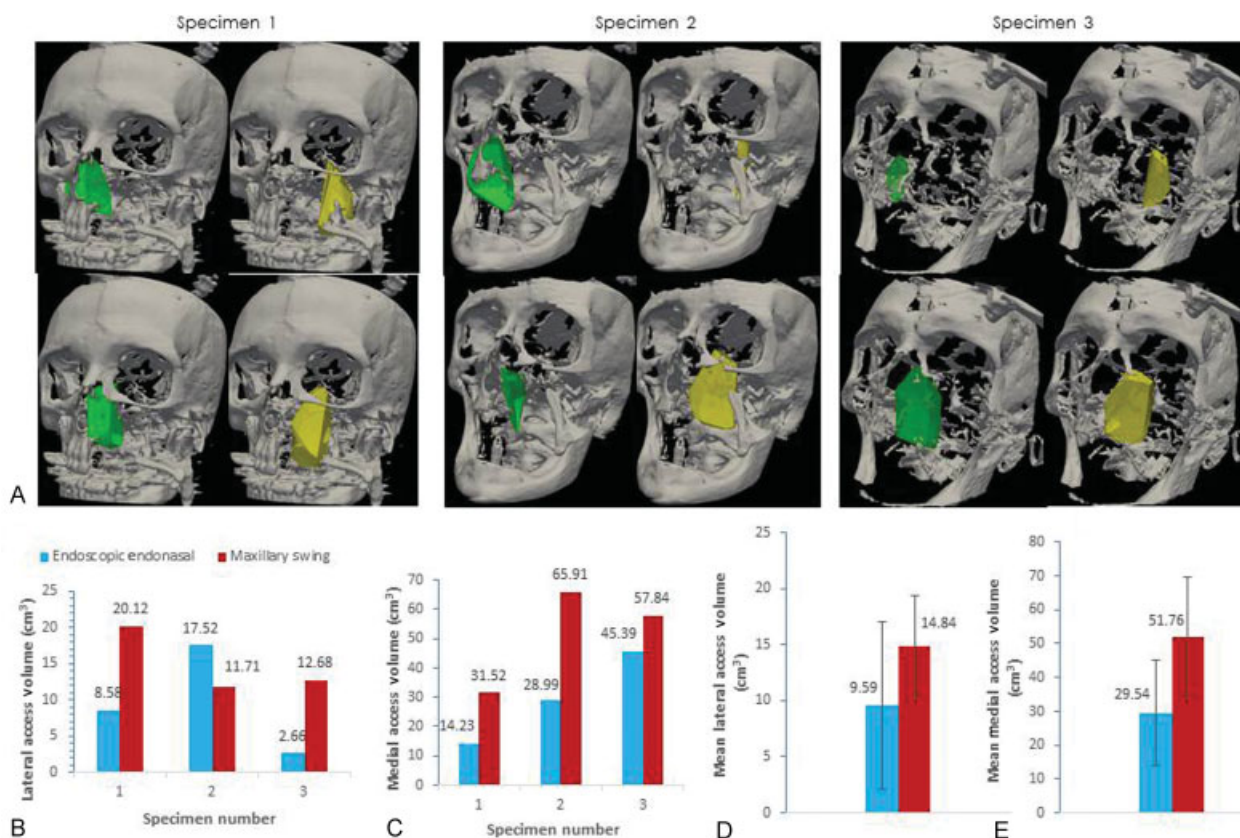


Fig. 5 (A) Lateral and medial split volumes for endonasal endoscopic approach (EEA) and maxillary swing (MS) approach. For each specimen: top left—EEA lateral; bottom left—EEA medial. Top right—MS lateral; bottom right—MS medial. (B) Lateral access volumes. (C) Medial access volumes. (D) Mean lateral access volume and standard deviation. (E) Mean medial access volume and standard deviation

superior anatomical structures such as delineation of the cavernous and paraclival carotid artery while using the endoscopic approach to nasopharyngectomy.

The MS provided a larger volume of exposure for surgical instrumentation and manipulation in comparison to EEA nasopharyngectomy (►Fig. 3). MS gains an average volume of 70% over the EEA. The mean access volume of the EEA and MS approaches is (66.6 cm³ +/- 13.4 vs 39.1 cm³ +/- 14.15, *p* = 0.009, *n* = 3). In addition, the deep surface area of exposure to the nasopharynx was also higher using the MS approach (54.2cm² +/- SD 5.5 vs 34.5 cm² +/- SD 12.25, *p* = 0.06, *n* = 3) (►Fig. 6B). The deep surface area for each specimen is illustrated in ►Fig. 3B. Similarly, the working surface area also exhibits a comparable trend where the MS approach had greater surface area exposure compared with the EEA approach (80.16 cm² +/- SD 8.11 vs 56.91 cm² +/- SD 17.66, *p* = 0.0646, *n* = 3) (►Fig. 6C).

The surface areas of exposure to the parapharyngeal internal carotid arteries were observed to be marginally higher in the MS approach in comparison to EEA (1.9 cm² +/- SD 0.07 vs 1.6 cm² +/- SD 0.09, *p* = 0.04, *n* = 2) (►Fig. 7A). ►Fig. 7B shows an illustration of the right and left internal carotid arteries, which were exposed using the EEA and MS approaches, respectively. The additional exposure to the parapharyngeal internal carotid artery was gained through a maxillary swing approach (MSA) mainly

through exposure of the artery below the hard palate gained through splitting the palate.

Both EEA and MS had greater medial volumes than lateral (EEA: 29.54 cm³ +/- 15.59 vs 9.59 cm³ +/- 7.48, *p* = 0.2253, *n* = 3 and MS: 51.76 cm³ +/- 17.98 vs 14.84 cm³ +/- 4.60, *p* = 0.1052, *n* = 3). Both EEA and MS had greater superior volumes than inferior across the soft palate split (EEA: 32.86 cm³ +/- 12.17 vs 6.26 cm³ +/- 9.23, *p* = 0.1059, *n* = 3 and MS: 58.11 cm³ +/- 18.86 vs 8.47 cm³ +/- 7.50, *p* = 0.0772, *n* = 3).

Discussion

In the current study, three adult cadaver specimens with arterial latex injection were used to compare surgical access using two different approaches to nasopharyngectomy: (1) an expanded EEA and (2) an open MS approach. While computer modeling of access volume has been reported, to our knowledge, this study is the first cadaveric study to quantitatively compare surgical access using two surgical approaches to the nasopharynx.²⁷

The quantitative data obtained from this study enables an objective assessment of the EEA for nasopharyngectomy, in terms of accessible volumes of exposure and working surface area to the nasopharynx and adjacent structures. The current study suggests that an endoscopic approach to

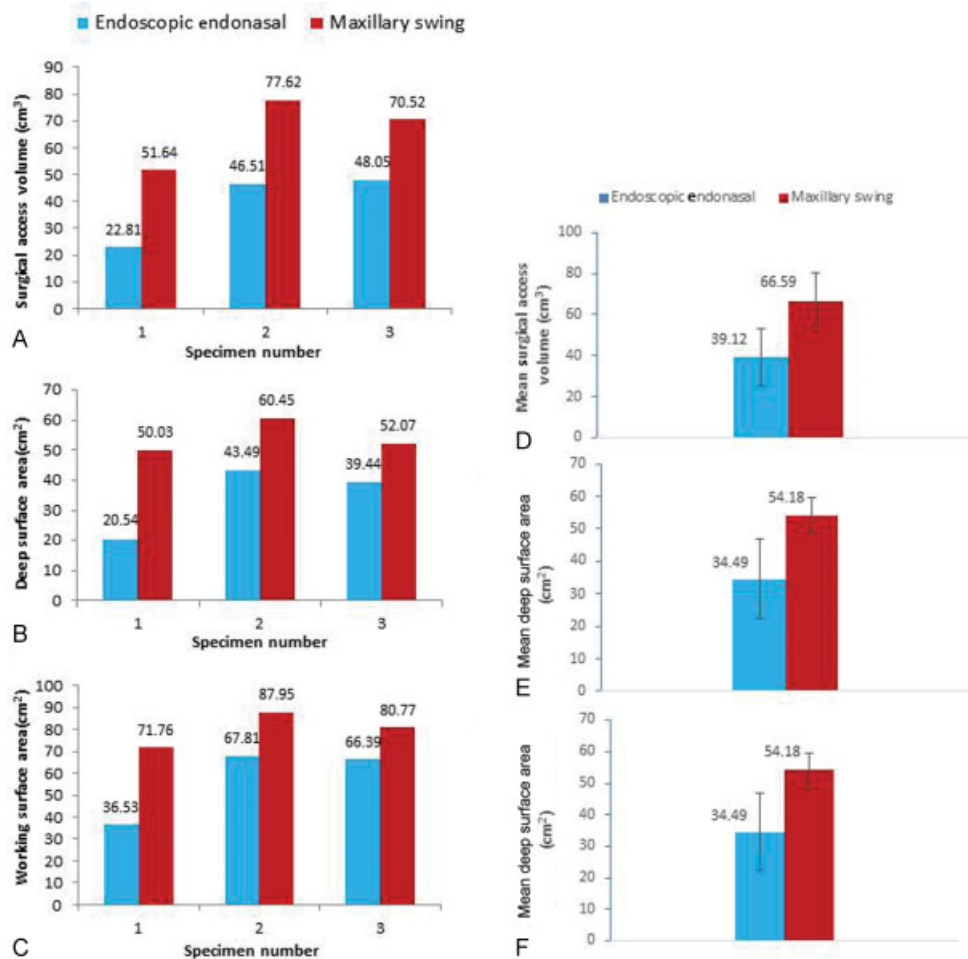


Fig. 6 (A) Surgical access volumes. (B) Deep surface area for endoscopic endonasal and maxillary swing approaches. (C) Working surface area for both surgical approaches. (D) Mean volume and standard deviation for both approaches. (E) Mean deep surface area and standard deviation for both approaches. (F) Mean working surface area and standard deviation for both approaches.

nasopharyngectomy provides adequate access and better visualization of superior anatomical structures such as delineation of the cavernous and paraclival carotid artery. The finding suggests that a MS approach provides increased working area and surgical access particularly in the patients with parapharyngeal extension may be better served with an MS approach. In particular, patients who have inferior extension via the parapharyngeal space to the region below the level of the palate, an EEA approach may not readily access this region. However, further adjuncts such as transoral combined with transnasal approaches may better address this region. For tumors with extensive lateral extension, further adjunctive procedures may improve lateral access. Denkers modifications to the EEA approach or a Caldwell-Luc approach may significantly improve lateral access when combined with the EEA. However, for patients with tumors confined to the nasopharynx or minimal lateral and inferior parapharyngeal space involvement, an EEA approach may be more than adequate.

Despite the improved surgical access with the MS approach, it is associated with facial incisions, a risk of palatal fistula, risk for loss of sensation in the infraorbital nerve distribution, and wound dehiscence and breakdown. The MS

approach also usually requires a tracheostomy to prevent airway obstruction. The endoscopic approach, on the other hand, is associated with low morbidity, short length of stay, and shorter procedure time and doesn't require any external incision. Given these potential advantages, it may be the ideal approach to appropriate patients. Our data would suggest that for central, superior, and posterior wall tumors the EEA approach maybe ideal.

We evaluated the working area in the region of the internal carotid artery particularly because surgical access to this major vessel may be important in cases with parapharyngeal extension. Understanding of the anatomy and proximity to the parapharyngeal ICA during nasopharyngectomy is essential to avoid potential catastrophic bleeding. Patients must be appropriately selected based on preoperative imaging to ensure potential clearance with margin control in the parapharyngeal space. Although our data would suggest that the MS approach provides higher surface area of exposure to the internal carotid arteries compared with the endoscopic approach, the visualization of this area was poor and the working area to manage hemorrhages was limited, although further anatomic studies in live animal models may better elucidate the benefits of surgical

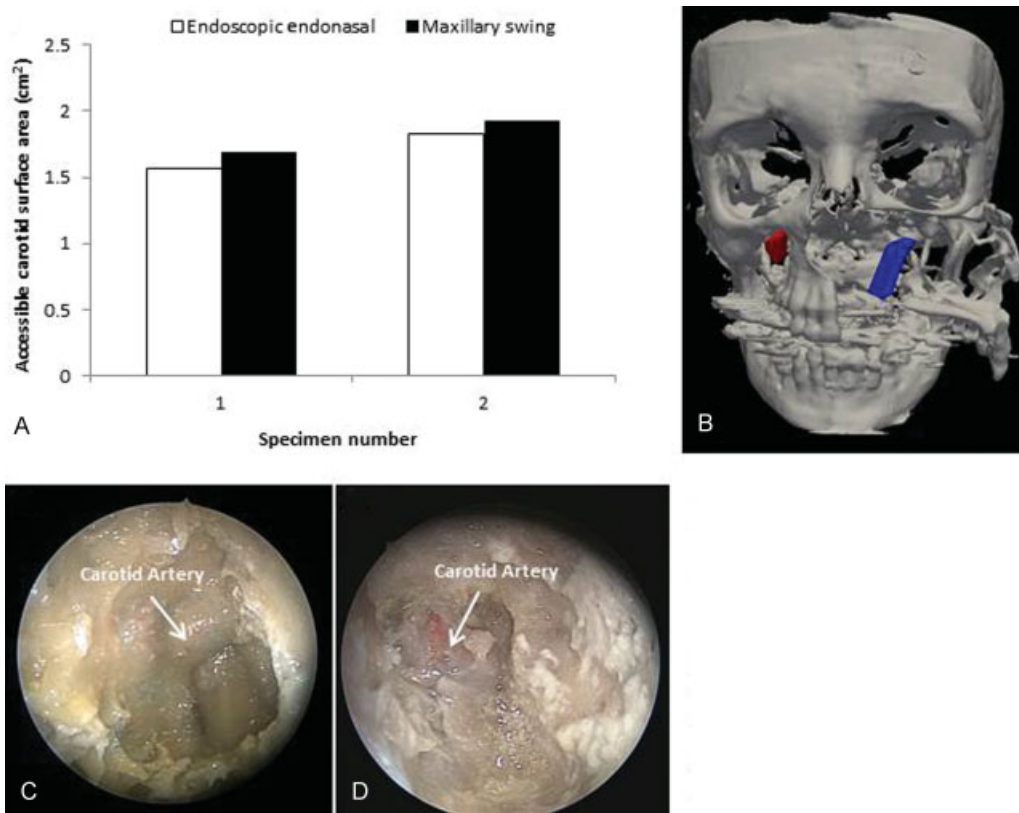


Fig. 7 (A) Accessible internal carotid artery surface area using the endoscopic endonasal and maxillary swing approaches. (B) Surfaces of left and right internal carotid arteries traced by the optical tracking system. (C) The internal carotid artery as visualized during the endoscopic procedure. (D) The internal carotid artery as visualized during the maxillary swing procedure.

approach in dealing with vascular catastrophes. Our results suggest that the access surface area to the parapharyngeal component of the internal carotid may be better with the MSA compared with the endoscopic approach, but this may not necessarily translate into surgical access for vascular control which is the important clinical need. Furthermore, we used a standard transpterygoid approach and did not perform further approaches for better access such as combining a transcervical approach, which often may be used complementarily with the EEA to ensure vessel control and also to better delineate the internal carotid in the parapharyngeal space to avoid injury during the endonasal portion of the procedure.

The use of navigation systems and quantitative analysis generated from navigated measurement is a novel application for the determination of surgical access. Navigated tools provide a way to qualitatively and quantitatively compare different surgical approaches. Navigated probes can accurately prescribe in real-time volume and surface area metrics that are representative of the surgical approach. Qualitatively, the clinician can see regions of overlap for different approaches that treat the same pathology as visualized in a 3D viewer. The clinical applicability of surgical access volumes is not clear. In this study, surgical access volume is used as a surrogate outcome for ease of the access to tumors and potential completeness of resection. The

approach for every tumor must be customized to the extent of the tumor, its precise location, and the merits of access granted by each of the surgical approaches studied. Furthermore, the use of angled scopes and instruments may in many cases expand the accessibility of tumors that is not fully captured in the surgical access volumes studied. Further studies are needed that address the completeness of resection with the different approaches.

In addition to volume and surface area metrics of an approach as traced by a tracked probe, tracking how surgical tools are used within the access volume would provide measures of surgical efficiency (ease of maneuver in a surgical access volume, how much volume / surface area is actually utilized, etc.) and should be incorporated in future studies. This would provide invaluable information that can help optimize surgical tool design and improve existing approaches.

This study has several limitations. We performed three cadaveric dissections and each cadaver may have considerable anatomic variability. As such, three specimens may not be an adequate representation of a comparison of the two approaches. In addition, we used tracking probes to measure surgical access volume comparing two approaches in a single cadaveric head with the endoscopic approach used on one side and the MSA on the contralateral side. In reality, the access volumes cross over the midline and this full access volume is not fully measured within the present study

because of the need to provide an internal control for the two approaches within each cadaveric head. Furthermore, the present study did not incorporate some relevant endpoints such as operative time, completeness of resection, and bleeding. These endpoints are relevant to patient care but may be difficult to measure in cadaveric studies. Lastly, surgical access volume, while important, may not adequately reflect the ability to maneuver surgical instruments and perform necessary tasks. Future cadaver studies with new endpoints are needed to better answer these questions.

References

- Al-Sarraf M, LeBlanc M, Giri PG, et al. Chemoradiotherapy versus radiotherapy in patients with advanced nasopharyngeal cancer: phase III randomized Intergroup study 0099. *J Clin Oncol* 1998;16(04):1310–1317
- Chan AT, Teo PM, Leung TW, Johnson PJ. The role of chemotherapy in the management of nasopharyngeal carcinoma. *Cancer* 1998;82(06):1003–1012
- Ma J, Mai HQ, Hong MH, et al. Results of a prospective randomized trial comparing neoadjuvant chemotherapy plus radiotherapy with radiotherapy alone in patients with locoregionally advanced nasopharyngeal carcinoma. *J Clin Oncol* 2001;19(05):1350–1357
- Wolden SL, Zelefsky MJ, Kraus DH, et al. Accelerated concomitant boost radiotherapy and chemotherapy for advanced nasopharyngeal carcinoma. *J Clin Oncol* 2001;19(04):1105–1110
- Lin JC, Jan JS, Hsu CY, Liang WM, Jiang RS, Wang WY. Phase III study of concurrent chemoradiotherapy versus radiotherapy alone for advanced nasopharyngeal carcinoma: positive effect on overall and progression-free survival. *J Clin Oncol* 2003;21(04):631–637
- Ridge JA. Squamous cancer of the head and neck: surgical treatment of local and regional recurrence. *Semin Oncol* 1993;20(05):419–429
- Teo PML, Kwan WH, Chan ATC, Lee WY, King WW, Mok CO. How successful is high-dose (> or = 60 Gy) reirradiation using mainly external beams in salvaging local failures of nasopharyngeal carcinoma? *Int J Radiat Oncol Biol Phys* 1998;40(04):897–913
- Wei WI, Sham JS. Nasopharyngeal carcinoma. *Lancet* 2005;365(9476):2041–2054
- King WWK, Ku PKM, Mok CO, Teo PM. Nasopharyngectomy in the treatment of recurrent nasopharyngeal carcinoma: a twelve-year experience. *Head Neck* 2000;22(03):215–222
- Fee WE Jr, Moir MS, Choi EC, Goffinet D. Nasopharyngectomy for recurrent nasopharyngeal cancer: a 2- to 17-year follow-up. *Arch Otolaryngol Head Neck Surg* 2002;128(03):280–284
- Wei WI, Lam KH, Sham JS. New approach to the nasopharynx: the maxillary swing approach. *Head Neck* 1991;13(03):200–207
- Becker AM, Hwang PH. Endoscopic endonasal anatomy of the nasopharynx in a cadaver model. *Int Forum Allergy Rhinol* 2013;3(04):319–324
- Al-Sheibani S, Zanation AM, Carrau RL, et al. Endoscopic endonasal transpterygoid nasopharyngectomy. *Laryngoscope* 2011;121(10):2081–2089
- Wen YH, Wen WP, Chen HX, Li J, Zeng YH, Xu G. Endoscopic nasopharyngectomy for salvage in nasopharyngeal carcinoma: a novel anatomic orientation. *Laryngoscope* 2010;120(07):1298–1302
- Yoshizaki T, Wakisaka N, Muroso S, Shimizu Y, Furukawa M. Endoscopic nasopharyngectomy for patients with recurrent nasopharyngeal carcinoma at the primary site. *Laryngoscope* 2005;115(08):1517–1519
- Chen MY, Wen WP, Guo X, et al. Endoscopic nasopharyngectomy for locally recurrent nasopharyngeal carcinoma. *Laryngoscope* 2009;119(03):516–522
- Ko JY, Wang CP, Ting LL, Yang TL, Tan CT. Endoscopic nasopharyngectomy with potassium-titanyl-phosphate (KTP) laser for early locally recurrent nasopharyngeal carcinoma. *Head Neck* 2009;31(10):1309–1315
- Castellnuovo P, Dallan I, Bignami M, et al. Nasopharyngeal endoscopic resection in the management of selected malignancies: ten-year experience. *Rhinology* 2010;48(01):84–89
- To EW, Yuen EH, Tsang WM, et al. The use of stereotactic navigation guidance in minimally invasive transnasal nasopharyngectomy: a comparison with the conventional open transfacial approach. *Br J Radiol* 2002;75(892):345–350
- Feldkamp LA, Davis LC, Kress JW. Practical cone-beam algorithm. *J Opt Soc Am A* 1984;1(06):612–619
- Enquobahrie A, Cheng P, Gary K, et al. The image-guided surgery toolkit IGSTK: an open source C++ software toolkit. *J Digit Imaging* 2007;20(Suppl 1):21–33
- Schroeder W, Martin K, Lorensen B. *Visualization Toolkit: An Object-Oriented Approach to 3D Graphics*, 4th Edition. New York, NY: Kitware; 2006
- Yoo TS. *Insight into Images: Principles and Practice for Segmentation, Registration, and Image Analysis*. Natick, MA: Taylor & Francis; 2004
- Alyassin AM, Lancaster JL, Downs JH III, Fox PT. Evaluation of new algorithms for the interactive measurement of surface area and volume. *Med Phys* 1994;21(06):741–752
- Weersink RA, Qiu J, Hope AJ, et al. Improving superficial target delineation in radiation therapy with endoscopic tracking and registration. *Med Phys* 2011;38(12):6458–6468
- King E, Daly MJ, Chan H, et al. Intraoperative cone-beam CT for head and neck surgery: feasibility of clinical implementation using a prototype mobile C-arm. *Head Neck* 2013;35(07):959–967
- Kapucu B, Gun R, Kirsch C, et al. Volumetric analysis of nasopharyngectomy via endoscopic endonasal, maxillary transposition, and lateral temporal-subtemporal approaches. *J Craniofac Surg* 2015;26(07):2136–2141